JOURNAL OF COMPUTATIONAL PHYSICS **128,** 341–350 (1996)
ARTICLE NO. 0215

Numerical Simulation of the (Nonlinear) Conduction/Radiation Heat Transfer Process in a Nonconvex and Black Cylindrical Body

ROGÉRIO MARTINS SALDANHA DA GAMA

Laboratório Nacional de Computação Científica, Rua Lauro Müller 455, 22290, Rio de Janeiro, Brazil

Received January 18, 1996; revised May 16, 1996

In this work the coupled conduction/radiation heat transfer process in a nonconvex and black cylindrical body is simulated. This nonlinear process is mathematically described by a partial differential equation subjected to a nonlinear boundary condition that represents the coupling between the conduction heat transfer and the thermal radiation heat transfer on a body boundary. The solution of the problem is reached as the limit of a sequence whose elements are obtained from the minimization of a functional. In this work the elements of this sequence are approximated by finite elements. Some particular cases are simulated and the results are compared with the ones obtained under the (usual) constant temperature hypothesis.

1. INTRODUCTION

The mechanism for energy transfer in bodies surrounded by an atmosphere-free space is a combination of conductive heat transfer and thermal radiative heat transfer [1]. For nonopaque bodies this combination takes place in the entire body [2, 3] but, if the body is opaque, the coupling between conduction and radiation occurs only on body boundary [4, 5].

The subject of this work is the energy transfer process in a rigid, opaque and nonconvex body surrounded by an atmosphere-free space.

This coupled conduction/radiation heat transfer process is an inherently nonlinear phenomenon, where the coupling between conduction and radiation on the body boundary is mathematically represented by a nonlinear relation between the absolute temperature and its exterior normal derivative. The unknown is the temperature distribution in the body.

When the heat transfer process takes place in a nonconvex body, the mathematical description becomes considerably more complex, since there will exist a direct thermal radiant interchange among subsets of body boundary. This interchange plays the role of a nonlinear temperature-dependent external source. In other words, the external energy supply on body boundary depends on the temperature field of this same body.

The inherent nonlinearity associated with nonconvexity gives rise to a class of complex and interesting mathematical problems, which is the main subject of this work, with a broad range of applications.

The main objective of this work is the (local) simulation of the steady-state conduction/radiation energy transfer process in a nonconvex body surrounded by vacuum, employing a systematic procedure which is reliable and adequate to the simulation of any conduction/radiation heat transfer problem in black bodies, and which provides only physically admissible solutions [4].

The simulation of energy transfer processes involving thermal radiation is in general carried out with the aid of several simplified approaches. The most common is the constant temperature approximation [6–8] in which the body is assumed to be isothermal. The linearized approach, where it is assumed the existence of a radiation heat transfer coefficient, is also usual, especially when there exists a convective heat transfer too [9].

In order to present concrete results to illustrate the effect of the nonconvexity and the consequences of the usual constant temperature approximation, the energy transfer process in a rigid and nonconvex (cylindrical) body will be considered. The body will be represented by the set

$$\Omega \equiv \{(x, y, z) \in \mathbb{R}^3 \text{ such that } R_1^2 < x^2 + y^2 < R_2^2, -L < z < L\}$$

with boundary $\partial\Omega \equiv \partial\Omega_1 \cup \partial\Omega_2 \cup \partial\Omega_U \cup \partial\Omega_L$ in which

$$\partial\Omega_1 \equiv \{(x, y, z) \in \mathbb{R}^3 \text{ such that } x^2 + y^2 = R_1^2, -L < z < L\}$$

$$\partial\Omega_2 \equiv \{(x, y, z) \in \mathbb{R}^3 \text{ such that } x^2 + y^2 = R_2^2, -L < z < L\}$$

$$\partial\Omega_U \cup \partial\Omega_L \equiv \{(x, y, z) \in \mathbb{R}^3 \text{ such that } R_1^2 < x^2 + y^2 < R_2^2 \text{ and } z = -L \text{ or } z = L\}$$

as it is represented in Fig. 1.

In order to simplify the mathematical problem the body will be assumed black (the black body does not reflect

0021-9991/96 $18.00

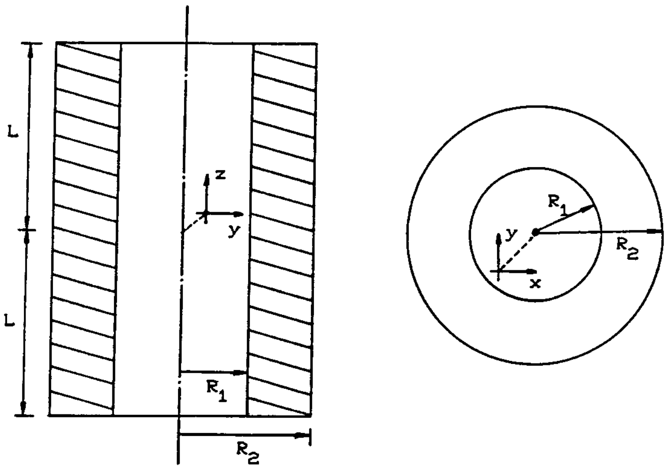

FIG. 1. The considered body.

thermal radiant energy). The black body assumption is physically reasonable for surfaces with high emittance (e.g., wrought iron oxidized $\rightarrow \varepsilon = 0.94$, silica $\rightarrow \varepsilon = 0.85$, black lacquer paint $\rightarrow \varepsilon = 0.93$) because these surfaces absorb almost all the incident thermal radiant energy [6].

It will be assumed that the body dissipates energy (for instance, due to the presence of electronic devices). This effect will be modelled as a source term in the partial differential equation which governs the heat transfer inside Ω.

Since the subset $\partial\Omega_1 \subset \partial\Omega$ is not convex the thermal radiant energy leaving $\partial\Omega_1$ can reach, directly, $\partial\Omega_1$. In other words, each point $(x, y, z) \in \partial\Omega_1$ is heated by a part of the thermal radiant energy which leaves $\partial\Omega_1$. This temperature-dependent effect, taken into account in the boundary conditions, increases the effort needed for simulating the problem.

A numerical simulation for this problem employing a finite element approximation will be presented. The results obtained will be compared with the ones obtained under the assumption of constant temperature.

The solution to the problem is given by the limit of a sequence whose elements are obtained from the minimization of functionals that are different from the usual ones employed in mechanics. They are not quadratic. Each of these elements represents the solution of a conduction/radiation heat transfer problem with a prescribed external thermal radiant source (instead of a temperature-dependent thermal radiant source). The limit of the sequence is the solution of the considered problem with a temperature-dependent thermal radiant source [4].

2. RADIATIVE TRANSFER FROM/TO $\partial\Omega$

According to the Stefan–Boltzmann law, the amount of thermal radiant energy (per unit time and unit area) emitted at a given point $(x, y, z) \in \partial\Omega$ is given by [1, 6]

$$E = \sigma T^4, \quad T = \hat{T}(x, y, z), \quad (x, y, z) \in \partial\Omega \tag{1}$$

in which σ is the Stefan–Boltzmann constant and T is the absolute temperature field. On physical grounds, T must be nonnegative everywhere.

Since the subsets $\partial\Omega_2$, $\partial\Omega_U$, and $\partial\Omega_L$ cannot receive thermal radiant energy from the body, the heat loss (per unit time and unit area) is given by

$$q_{\text{rad}} = \sigma T^4, \quad T = \hat{T}(x, y, z), \quad (x, y, z) \in \partial\Omega_2 \cup \partial\Omega_U \cup \partial\Omega_L. \tag{2}$$

The heat loss from $\partial\Omega_1$ is not given by (2), since the energy leaving this surface will, in part, reach itself. Hence, the heat loss from $\partial\Omega_1$ is given by the difference between the emitted thermal radiant energy (given by (1)) and the incident thermal radiant energy on $\partial\Omega_1$. In other words,

$$q_{\text{rad}} = \sigma T^4 - H, \quad T = \hat{T}(x, y, z), \quad H = \hat{H}(x, y, z), \quad (x, y, z) \in \partial\Omega_1 \tag{3}$$

in which H is the incident thermal radiant energy per unit time and unit area on $\partial\Omega_1$.

The field H is given by [1]

$$H = \hat{H}(x, y, z) = \int_{(x',y',z')\in\partial\Omega_1} \sigma \hat{T}(x', y', z')^4 \hat{K}(x, y, z, x', y', z')\, dS', \quad (x, y, z) \in \partial\Omega_1 \tag{4}$$

in which, assuming that T depends only on z and r ($r \equiv (x^2 + y^2)^{1/2}$ is the radial variable), the kernel $\hat{K}(x, y, z, x', y', z')$ may be expressed as

$$\hat{K}(x, y, z, x', y', z') = \frac{1}{4\pi R_1^2}\left[1 - |z - z'|\left(\frac{(z - z')^2 + 6R_1^2}{[(z - z')^2 + 4R_1^2]^{3/2}}\right)\right] \tag{5}$$

for $(x, y, z) \in \partial\Omega_1$ and $(x', y', z') \in \partial\Omega_1$

3. CONDUCTION HEAT TRANSFER INSIDE Ω

Since the body is rigid and opaque (black) the energy transfer mechanism inside Ω is conductive heat transfer. The steady-state conductive heat transfer in Ω is governed by [10]

$$-\operatorname{Div} \mathbf{q} + \mathring{q} = 0, \quad \mathbf{q} = -k \operatorname{Grad} T, \quad (x, y, z) \in \Omega \tag{6}$$

in which $\mathbf{q}$ is the conduction heat flux per unit time and unit area, k is the thermal conductivity (assumed constant), and $\mathring{q}$ is the internal energy supply per unit time and unit volume (assumed constant and positive).

4. THE COUPLED CONDUCTION/RADIATION HEAT TRANSFER

The mathematical description for the considered heat transfer process is obtained when (6) is regarded, together with the continuity in the normal heat flux on $\partial\Omega$.

Since $\mathring{q}/k$ is a constant and the body is cylindrical, it seems to be more convenient to work with cylindrical coordinates. Hence, taking into account the radial symmetry, the mathematical problem may be represented as

$$\begin{aligned}
&\frac{1}{r}\frac{\partial}{\partial r}\left(r\frac{\partial T}{\partial r}\right)+\frac{\partial^2 T}{\partial z^2}+\frac{\mathring{q}}{k}=0, \quad R_1<r<R_2, 0<z<L,\\
&-k\frac{\partial T}{\partial r}=\sigma T^4 \quad \text{for } r=R_2, 0<z<L,\\
&\frac{\partial T}{\partial z}=0 \quad \text{for } z=0, R_1<r<R_2,\\
&-k\frac{\partial T}{\partial z}=\sigma T^4 \quad \text{for } z=L, R_1<r<R_2,\\
&k\frac{\partial T}{\partial r}=\sigma T^4-\int_0^L \sigma\tilde{T}(R_1,z')^4(\tilde{K}(z,z')+\tilde{K}(z,-z'))\\
&2\pi R_1\,dz' \quad \text{for } r=R_1, 0<z<L.
\end{aligned} \tag{7}$$

5. DIMENSIONLESS FORMULATION

At this point it is convenient to introduce the definitions

$$\xi=\frac{r}{L}; \quad \eta=\frac{z}{L} \tag{9}$$

$$\gamma_1=\frac{R_1}{L}; \quad \gamma_2=\frac{R_2}{L}; \frac{1}{\alpha}=\frac{k^4}{\sigma\mathring{q}^3L^7} \tag{10}$$

$$\theta=\left(\frac{k}{\mathring{q}L^2}\right)T \tag{11}$$

and rewrite problem (7) as

$$\begin{aligned}
&\frac{1}{\xi}\frac{\partial}{\partial \xi}\left(\xi\frac{\partial \theta}{\partial \xi}\right)+\frac{\partial^2 \theta}{\partial \eta^2}+1=0, \quad \gamma_1<\xi<\gamma_2, 0<\eta<1,\\
&-\frac{\partial\theta}{\partial\xi}=\alpha\theta^4 \quad \text{for } \xi=\gamma_2, 0<\eta<1,\\
&\frac{\partial\theta}{\partial\eta}=0 \quad \text{for } \eta=0, \gamma_1<\xi<\gamma_2,\\
&-\frac{\partial\theta}{\partial\eta}=\alpha\theta^4 \quad \text{for } \eta=1, \gamma_1<\xi<\gamma_2,\\
&\frac{\partial\theta}{\partial\xi}=\alpha\theta^4-\int_0^1\alpha\tilde{\theta}(R_1,\eta')^4K^*(\eta,\eta')\,d\eta'\\
&\qquad \text{for } \xi=\gamma_1, 0<\eta<1,
\end{aligned} \tag{12}$$

in which $\theta=\tilde{\theta}(\xi,\eta)$ and

$$K^*(\eta,\eta')=\frac{1}{2\gamma_1}\left\{2-|\eta-\eta'|\left(\frac{(\eta-\eta')^2+6\gamma_1^2}{[(\eta-\eta')^2+4\gamma_1^2]^{3/2}}\right)-|\eta+\eta'|\left(\frac{(\eta+\eta')^2+6\gamma_1^2}{[(\eta+\eta')^2+4\gamma_1^2]^{3/2}}\right)\right\}. \tag{13}$$

6. CONSTRUCTION OF THE SOLUTION

The solution, θ, to (12) is the limit of the sequence $[\Psi^0, \Psi^1, \Psi^2, \Psi^3, ...]$. The term Ψ^p ($\Psi^p=\hat{\Psi}^p(\xi,\eta)$) is obtained from the minimization of the functional $I^p[u]$ given by [4]

$$\begin{aligned}
I^p[u]&=\frac{1}{2}\int_{\gamma_1}^{\gamma_2}\int_0^1\left[\left(\frac{\partial u}{\partial\xi}\right)^2+\left(\frac{\partial u}{\partial\eta}\right)^2\right]\xi d\eta\,d\xi-\int_{\gamma_1}^{\gamma_2}\int_0^1 u\xi\,d\eta\,d\xi\\
&+\frac{1}{5}\left[\int_{\gamma_1}^{\gamma_2}\alpha|u|^5\xi d\xi\right]_{\eta=1}+\frac{1}{5}\left[\int_0^1\alpha|u|^5\xi d\eta\right]_{\xi=\gamma_2}\\
&+\frac{1}{5}\left[\int_0^1\alpha|u|^5\xi\,d\eta\right]_{\xi=\gamma_1}-\left[\int_0^1 h^p u\xi\,d\eta\right]_{\xi=\gamma_1}
\end{aligned} \tag{14}$$

in which

$$h^p=\hat{h}^p(\eta)=\int_0^1\alpha[\hat{\Psi}^{p-1}(\gamma_1,\eta')]^4K^*(\eta,\eta')\,d\eta' \tag{15}$$

with $\Psi^0\equiv 0$.

Taking the first variation of $I^p[u]$, the following Euler–Lagrange equation and natural boundary conditions are obtained,

$$\begin{aligned}
&\frac{1}{\xi}\frac{\partial}{\partial\xi}\left(\xi\frac{\partial\Psi^p}{\partial\xi}\right)+\frac{\partial^2\Psi^p}{\partial\eta^2}+1=0, \quad \gamma_1<\xi<\gamma_2, 0<\eta<1,\\
&-\frac{\partial\Psi^p}{\partial\xi}=\alpha|\Psi^p|^3\Psi^p \quad \text{for } \xi=\gamma_2, 0<\eta<1,\\
&\frac{\partial\Psi^p}{\partial\eta}=0 \quad \text{for } \eta=0, \gamma_1<\xi<\gamma_2,\\
&-\frac{\partial\Psi^p}{\partial\eta}=\alpha|\Psi^p|^3\Psi^p \quad \text{for } \eta=1, \gamma_1<\xi<\gamma_2,\\
&\frac{\partial\Psi^p}{\partial\xi}=\alpha|\Psi^p|^3\Psi^p-\int_0^1\alpha[\hat{\Psi}^{p-1}(\gamma_1,\eta')]^4K^*(\eta,\eta')\,d\eta'\\
&\qquad \text{for } \xi=\gamma_1, 0<\eta<1,
\end{aligned} \tag{16}$$

in which the (weak) solution Ψ^p minimizes $I^p[u]$.

Since $\alpha>0$ and

$$\int_0^1 K^*(\eta,\eta')\,d\eta'<1 \quad \text{for any } \eta\in[0,1] \tag{17}$$

the sequence $[\Psi^0, \Psi^1, \Psi^2, ...]$ is such that

$$\hat{\Psi}^p(\xi,\eta) \geq \hat{\Psi}^{p-1}(\xi,\eta) \geq \cdots > \hat{\Psi}^1(\xi,\eta) \geq 0; \quad \gamma_1 < \xi < \gamma_2, 0 < \eta < 1, \tag{18}$$

and has as its limit a nonnegative function (denoted here by Ψ^∞) that is the unique solution of (12). In other words $\theta \equiv \Psi^\infty$ is the unique solution of problem (12) [11].

Hence, the solution of (12) (denoted here by θ) may be reached through the minimization of the functionals $I^1[u]$, $I^2[u]$, $I^3[u]$, ... defined by (14). This assertion is proved in [4].

7. THE CONSTANT TEMPERATURE APPROXIMATION

Frequently, for engineering purposes energy transfer problems like the one considered here are regarded under the assumption that the body temperature is constant. This approximation may be reached by assuming that the admissible fields u are constant (when minimizing $I^p[u]$).

The constant temperature approximation θ_c will be the limit of the sequence $[\Psi_c^0, \Psi_c^1, \Psi_c^2, \Psi_c^3, ...]$ (in which $\Psi_c^0 = 0$) whose elements are given by

$$\Psi_c^p = \left\{ \frac{\gamma_2^2 - \gamma_1^2 + \alpha[2\gamma_1 - 2(\gamma_1^2+1)^{1/2} + 2](\Psi_c^{p-1})^4}{\alpha[\gamma_2^2 - \gamma_1^2 + 2\gamma_2 + 2\gamma_1]} \right\}^{1/4}. \tag{19}$$

In this case the limit of the sequence is given by

$$\theta_c = \lim_{p\to\infty} \Psi_c^p = \left\{ \frac{\gamma_2^2 - \gamma_1^2}{\alpha[\gamma_2^2 - \gamma_1^2 + 2\gamma_2 + 2(\gamma_1^2+1)^{1/2} - 2]} \right\}^{1/4}. \tag{20}$$

These results will be used for comparisons with other approximations (to be constructed by finite elements).

8. THE FINITE ELEMENT APPROXIMATION

The first step for reaching a finite element approximation for the dimensionless temperature field θ is to look for an approximation for the elements of the sequence $[\Psi^0, \Psi^1, \Psi^2, ...]$.

The following finite element approximation will be considered for the admissible fields u, for each cell j, when minimizing $I^p[u]$ (see Fig. 2),

$$u = \begin{cases} (u_{i+1}^p - u_i^p)\phi + u_{i+1+M}^p - (u_{i+1+M}^p - u_i^p)\nu \\ \qquad \text{for } 0 \leq \phi \leq 1, \phi \leq \nu \leq 1, \\ (u_{i+2+M}^p - u_{i+1+M}^p)\phi + u_{i+1+M}^p + (u_{i+1}^p - u_{i+2+M}^p)\nu \\ \qquad \text{for } 0 \leq \phi \leq 1, 0 \leq \nu \leq \phi, \end{cases}$$

$$i = j + \text{int}\left(\frac{j-1}{M}\right), j = 1, 2, 3, ..., NM. \tag{21}$$

In the above equations M and N are such that $(M+1)$ and $(N+1)$ are, respectively, the number of nodes in the ξ and η directions and "int" denotes the "integer part of."

In (21) u_i^p is the value of the admissible field u at the node i.

Combining (14) with (21) the functional $I^p[u]$ becomes the function g^p given by

$$g^p = \hat{g}^p(u_1^p, u_2^p, ..., u_{(N+1)(M+1)}^p) = \sum_{j=1}^{NM} (A_j^p + B_j^p) + \sum_{j=1}^{M} C_j^p + \sum_{k=1}^{N} (D_k^p + E_k^p + F_k^p) \tag{22}$$

in which A_j^p, B_j^p, C_j^p, D_k^p, E_k^p, and F_k^p are given as

$$A_j^p = \frac{1}{2}\int_{\xi_j}^{\xi_j+\Delta\xi}\int_{\eta_j}^{\eta_j+\Delta\eta}\left[\left(\frac{\partial u}{\partial\xi}\right)^2 + \left(\frac{\partial u}{\partial\eta}\right)^2\right]\xi\, d\xi\, d\eta = \frac{1}{2}\Delta\xi\,\Delta\eta\int_0^1\int_0^1\left[\left(\frac{1}{\Delta\xi}\frac{\partial u}{\partial\phi}\right)^2 + \left(\frac{1}{\Delta\eta}\frac{\partial u}{\partial\nu}\right)^2\right](\xi_j + \phi\Delta\xi)\, d\nu\, d\phi,$$

$$j = 1, 2, 3, ..., NM; \tag{23}$$

$$B_j^p = -\int_{\xi_j}^{\xi_j+\Delta\xi}\int_{\eta_j}^{\eta_j+\Delta\eta} u\xi\, d\eta\, d\xi = -\Delta\xi\,\Delta\eta\int_0^1\int_0^1 u(\xi_j + \phi\Delta\xi)\, d\nu\, d\phi,$$

$$j = 1, 2, 3, ..., NM; \tag{24}$$

$$C_j^p = \frac{\alpha}{5}\left[\int_{\xi_j}^{\xi_j+\Delta\xi}|u|^5\xi\, d\xi\right]_{\eta=1} = \frac{\alpha}{5}\Delta\xi\left[\int_0^1|u|^5(\xi_j + \phi\Delta\xi)\, d\phi\right]_{\nu=1},$$

$$j = 1, 2, 3, ..., M; \tag{25}$$

$$D_k^p = \frac{\alpha}{5}\gamma_2\left[\int_{\eta_j}^{\eta_j+\Delta\eta}|u|^5\, d\eta\right]_{\xi=\gamma_2} = \frac{\alpha}{5}\gamma_2\,\Delta\eta\left[\int_0^1|u|^5\, d\nu\right]_{\phi=1},$$

$$k = \text{int}\left(\frac{j-1}{M}\right) + 1, j = M, 2M, 3M, ..., NM; \tag{26}$$

$$E_k^p = \frac{\alpha}{5}\gamma_1\left[\int_{\eta_j}^{\eta_j+\Delta\nu}|u|^5\, d\eta\right]_{\xi=\gamma_1} = \frac{\alpha}{5}\gamma_1\,\Delta\eta\left[\int_0^1|u|^5\, d\nu\right]_{\phi=0},$$

$$k = \text{int}\left(\frac{j-1}{M}\right) + 1, j = 1, M+1, 2M+1, ..., (N-1)M+1; \tag{27}$$

$$F_k^p = -\gamma_1\left[\int_{\eta_j}^{\eta_j+\Delta\eta}h^p u\, d\eta\right]_{\xi=\gamma_1} = -\gamma_1\,\Delta\eta\left[\int_0^1 h_k^p u\, d\nu\right]_{\phi=0},$$

$$k = \text{int}\left(\frac{j-1}{M}\right) + 1, j = 1, M+1, 2M+1, ..., (N-1)M+1. \tag{28}$$

In (28) the field h_k^p is defined as

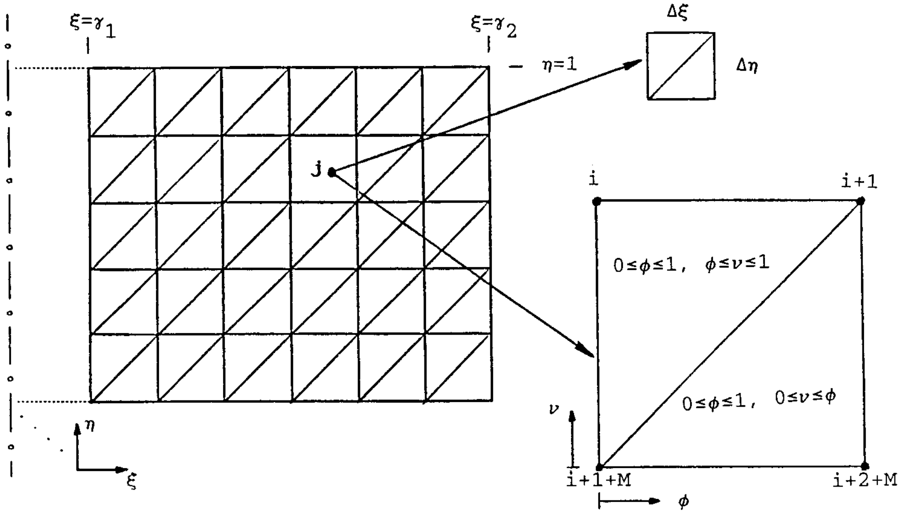

FIG. 2. The considered finite element approximation and a typical cell j (with elements $2j-1$ and $2j$).

$$h_k^p = \hat{h}_k^p(\nu) = \hat{h}^p(1-(k-\nu)\,\Delta\eta), \qquad 0 \le \nu \le 1,\ k=1,2,3,\ldots,N. \tag{29}$$

From (23), (24), (25), (26), and (27) the expressions for A_j^p, B_j^p, C_j^p, D_k^p, and E_k^p are obtained,

$$A_j^p = \frac{1}{2}\Delta\xi\,\Delta\eta\left\{\left[\left(\frac{u_{i+1}^p - u_i^p}{\Delta\xi}\right)^2 + \left(\frac{u_i^p - u_{i+1+M}^p}{\Delta\eta}\right)^2\right]\left(\frac{1}{2}\xi_j + \frac{1}{6}\Delta\xi\right) + \left[\left(\frac{u_{i+2+M}^p - u_{i+1+M}^p}{\Delta\xi}\right)^2 + \left(\frac{u_{i+1}^p - u_{i+2+M}^p}{\Delta\eta}\right)^2\right]\left(\frac{1}{2}\xi_j + \frac{1}{3}\Delta\xi\right)\right\}, \quad j=1,2,3,\ldots,NM; \tag{30}$$

$$B_j^p = -\Delta\xi\,\Delta\eta\left\{(u_{i+1}^p - u_i^p)\left(\frac{1}{6}\xi_j + \frac{1}{12}\Delta\xi\right) - (u_{i+1+M}^p - u_i^p)\left(\frac{1}{3}\xi_j + \frac{1}{8}\Delta\xi\right) + u_{i+1+M}^p\left(\xi_j + \frac{1}{2}\Delta\xi\right) - (u_{i+2+M}^p - u_{i+1}^p)\left(\frac{1}{6}\xi_j + \frac{1}{8}\Delta\xi\right) + (u_{i+2+M}^p - u_{i+1+M}^p)\left(\frac{1}{3}\xi_j + \frac{1}{4}\Delta\xi\right)\right\}, \quad j=1,2,3,\ldots,NM; \tag{31}$$

$$C_j^p = \frac{\alpha}{5}\Delta\xi\left\{\xi_j\,\frac{|u_{j+1}^p|^5 u_{j+1}^p - |u_j^p|^5 u_j^p}{6(u_{j+1}^p - u_j^p)} + \Delta\xi\left[\frac{|u_{j+1}^p|^7 - |u_j^p|^7}{7(u_{j+1}^p - u_j^p)^2} - \frac{|u_{j+1}^p|^5 u_{j+1}^p - |u_j^p|^5 u_j^p}{6(u_{j+1}^p - u_j^p)^2}\,u_j\right]\right\}, \quad \text{if } u_{j+1}^p \ne u_j^p;$$

$$C_j^p = \frac{\alpha}{5}\Delta\xi\left(\xi_j + \frac{1}{2}\Delta\xi\right)|u_j^p|^5, \quad \text{if } u_j^p = u_{j+1}^p,\ j=1,2,3,\ldots,M; \tag{32}$$

$$D_k^p = \frac{\alpha}{5}\gamma_2\,\Delta\eta\left\{\frac{|u_{k(M+1)}^p|^5 u_{k(M+1)}^p - |u_{(k+1)(M+1)}^p|^5 u_{(k+1)(M+1)}^p}{6(u_{k(M+1)}^p - u_{(k+1)(M+1)}^p)}\right\}, \quad \text{if } u_{k(M+1)}^p \ne u_{(k+1)(M+1)}^p;$$

$$D_k^p = \frac{\alpha}{5}\gamma_2\,\Delta\eta\,|u_{k(M+1)}^p|^5, \quad \text{if } u_{k(M+1)}^p = u_{(k+1)(M+1)}^p,\ k=1,2,3,\ldots,N; \tag{33}$$

$$E_k^p = \frac{\alpha}{5}\gamma_1\,\Delta\eta\left\{\frac{|u_{(k-1)(M+1)+1}^p|^5 u_{(k-1)(M+1)+1}^p - |u_{k(M+1)+1}^p|^5 u_{k(M+1)+1}^p}{6(u_{(k-1)(M+1)+1}^p - u_{k(M+1)+1}^p)}\right\}, \quad \text{if } u_{(k-1)(M+1)+1}^p \ne u_{k(M+1)+1}^p;$$

$$E_k^p = \frac{\alpha}{5}\gamma_1\,\Delta\eta\,|u_{(k-1)(M+1)+1}^p|^5, \quad \text{if } u_{(k-1)(M+1)+1}^p = u_{k(M+1)+1}^p,\ k=1,2,3,\ldots,N; \tag{34}$$

while the evaluation of F_k^p will be discussed in the next section.

The approximation for Ψ^p is, in this case, given by

$$\Psi^p = \begin{cases} (\Psi^p_{i+1} - \Psi^p_i)\phi + \Psi^p_{i+1+M} - (\Psi^p_{i+1+M} - \Psi^p_i)\nu \\ \quad \text{for } 0 \le \phi \le 1, \phi \le \nu \le 1, \\ (\Psi^p_{i+2+M} - \Psi^p_{i+1+M})\phi + \Psi^p_{i+1+M} + (\Psi^p_{i+1} - \Psi^p_{i+2+M})\nu \\ \quad \text{for } 0 \le \phi \le 1, 0 \le \nu \le \phi, j = 1, 2, 3, ..., NM, \end{cases} \tag{35}$$

in which $\Psi^p_1, \Psi^p_2, \Psi^p_3, ..., \Psi^p_{(N+1)(M+1)-1}$ and $\Psi^p_{(N+1)(M+1)}$ are such that the minimum of g^p is given by $g^p_{\min} = \hat{g}^p(\Psi^p_1, \Psi^p_2, \Psi^p_3, ..., \Psi^p_{(N+1)(M+1)})$.

9. EVALUATING F^p_k

The term F^p_k will be given as

$$F^p_k = c^p_k(u^p_{(k-1)(M+1)+1} - u^p_{k(M+1)+1}) + d^p_k u^p_{k(M+1)+1}, \quad k = 1, 2, 3, ..., N. \tag{36}$$

The coefficients c^p_k and d^p_k are given by

$$c^p_k = -\gamma_1 \Delta\eta \int_0^1 h^p_k \nu \, d\nu, \quad d^p_k = -\gamma_1 \Delta\eta \int_0^1 h^p_k \, d\nu \tag{37}$$

in which

$$\begin{aligned} h^p_k = \hat{h}^p_k(\nu) = \hat{h}^p(1 - (k - \nu)\Delta\eta) &= \sum_{n=1}^{N} \int_0^1 f^p_{kn}(\nu, \nu') \, d\nu' \\ = \sum_{n=1}^{N} \int_0^1 \alpha[(\Psi^{p-1}_{(n-1)(M+1)+1} &- \Psi^{p-1}_{n(M+1)+1})\nu' \\ + \Psi^{p-1}_{n(M+1)+1}]^4 K^{**}_{kn}(\nu, \nu') \, d\nu', \\ 0 \le \nu \le 1, \; k = 1, 2, 3, ..., N, \end{aligned} \tag{38}$$

where $K^{**}_{kn}(\nu, \nu')$ is given as.

$$\begin{aligned} K^{**}_{kn}(\nu, \nu') = \Delta\eta \frac{1}{2\gamma_1} \Bigg\{ 2 &- |(\nu - \nu' + n - k)\Delta\nu| \\ &\left[\frac{((\nu - \nu' + n - k)\Delta\eta)^2 + 6\gamma_1^2}{[((\nu - \nu' + n - k)\Delta\eta)^2 + 4\gamma_1^2]^{3/2}} \right] \\ &- |(\nu + \nu' - n - k)\Delta\eta + 2| \\ &\left[\frac{((\nu + \nu' - n - k)\Delta\eta + 2)^2 + 6\gamma_1^2}{[((\nu + \nu' - n - k)\Delta\eta + 2)^2 + 4\gamma_1^2]^{3/2}} \right] \Bigg\}, \\ k = 1, 2, 3, ..., N; \; n = 1, 2, 3, ..., N. \end{aligned} \tag{39}$$

The coefficients c^p_k and d^p_k will be approximated by

$$\begin{aligned} c^p_k = \gamma_1 \Delta\eta \sum_{n=1}^{N} \bar{c}^p_{kn}, \quad \bar{c}^p_{kn} &= \sum_{\beta_1=1}^{L} \sum_{\beta_2=1}^{L} \\ \{(f^p_{kn}((\beta_1 - 1)\Delta\nu, &(\beta_2 - 1)\Delta\nu) \\ + f^p_{kn}((\beta_1 - 1)\Delta\nu, \beta_2\Delta\nu))(\beta_1 - 1)\Delta\nu \\ + (f^p_{kn}(\beta_1\Delta\nu, (\beta_2 - 1)\Delta\nu) \\ + f^p_{kn}(\beta_1\Delta\nu, \beta_2\Delta\nu))\beta_1\Delta\nu\} \left(\frac{1}{2}\Delta\nu\right)^2, \\ \Delta\nu = \frac{1}{L}, k = 1, 2, 3, ..., N; \end{aligned} \tag{40}$$

$$\begin{aligned} d^p_k = \gamma_1 \Delta\eta \sum_{n=1}^{N} \bar{d}^p_{kn}, \quad \bar{d}^p_{kn} &= \sum_{\beta_1=1}^{L} \sum_{\beta_2=1}^{L} \\ \{(f^p_{kn}((\beta_1 - 1)\Delta\nu, &(\beta_2 - 1)\Delta\nu) \\ + f^p_{kn}((\beta_1 - 1)\Delta\nu, \beta_2\Delta\nu) \\ + f^p_{kn}(\beta_1\Delta\nu, (\beta_2 - 1)\Delta\nu) \\ + f^p_{kn}(\beta_1\Delta\nu, \beta_2\Delta\nu)\} \left(\frac{1}{2}\Delta\nu\right)^2, \\ \Delta\nu = \frac{1}{L}, k = 1, 2, 3, ..., N; \end{aligned} \tag{41}$$

in which $(L + 1)$ is the number of nodes for the numerical integration.

10. THE PROCEDURE FOR MINIMIZING g^p

The coefficients Ψ^p_i in (35) are obtained from the minimization of the function g^p, with $(N + 1)(M + 1)$ independent real variables.

The procedure used for minimizing g^p consists of employing, successively, a Newton scheme [12] for minimizing the functions g^p_q, with one real variable.

Defining $(X^0_1, X^0_2, X^0_3, ..., X^0_{(N+1)(M+1)})$ as the initial estimate and $(X^m_1, X^m_2, X^m_3, ..., X^m_{(N+1)(M+1)})$ as the estimate at the iteration m for $(\Psi^p_1, \Psi^p_2, \Psi^p_3, ..., \Psi^p_{(N+1)(M+1)})$, the function g^p_q is defined as

$$g^p_q = \hat{g}^p_q(X) = \hat{g}^p(X^{m+1}_1, X^{m+1}_2, ..., X^{m+1}_{q-1}, X, X^m_{q+1}, ..., X^m_{(N+1)(M+1)}). \tag{42}$$

The minimum of g^p_q is obtained from the root of the (nonlinear) equation

$$\frac{dg^p_q}{dX} = 0, \quad g^p_q = \hat{g}^p_q(X). \tag{43}$$

The root of (43) is obtained from the (Newton) iterative scheme

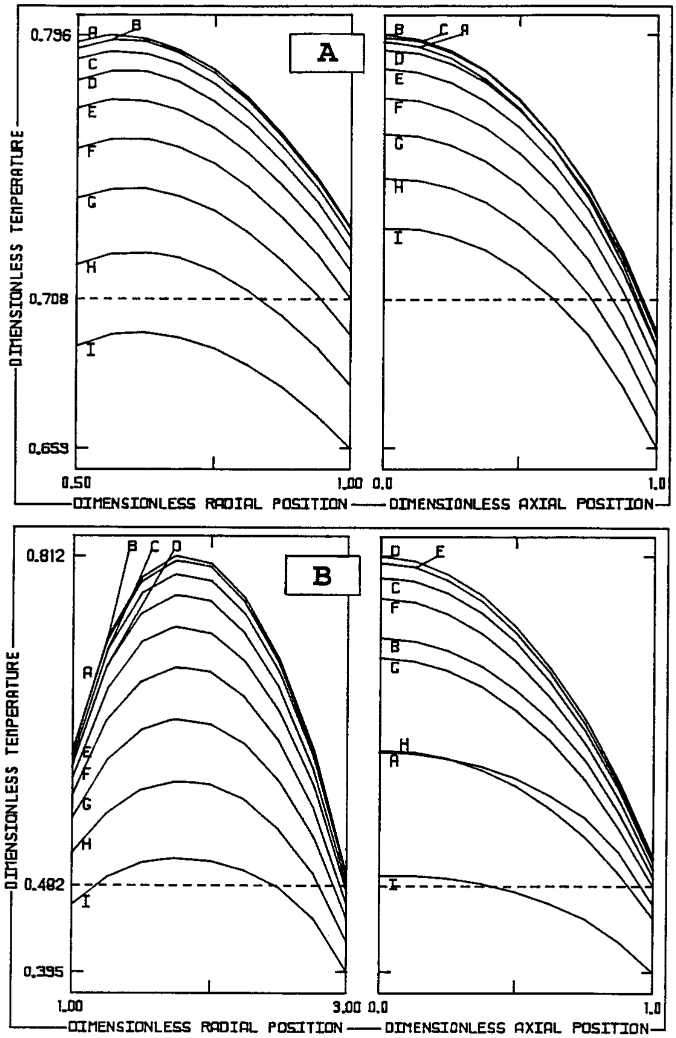

FIG. 3. Dimensionless temperature θ versus dimensionless radial position ξ (the curves A, B, ..., I correspond to $\eta = 0.000$, $\eta = 0.125$, ..., $\eta = 1.000$) and versus dimensionless axial position η (for part **A** the curves A, B, ..., I correspond to $\xi = 0.500$, $\xi = 0.5625$, ..., $\xi = 1.000$ and for part **B** the curves A, B, ..., I correspond to $\xi = 1.000$, $\xi = 1.250$, ..., $\xi = 3.000$). Obtained with $M = N = 8$ for $\alpha = 1.0$, $\gamma_1 = 0.5$, and $\gamma_2 = 1.0$ (part **A**) and for $\alpha = 10.0$, $\gamma_1 = 1.0$, and $\gamma_2 = 3.0$ (part **B**). The dashed line represents the constant temperature approximation.

$$Y^{\mu+1} = Y^{\mu} - \left.\frac{dg_q^p}{dX}\right|_{X=Y^{\mu}} \Bigg/ \left.\frac{d^2 g_q^p}{dX^2}\right|_{X=Y^{\mu}} \tag{44}$$

in which

$$Y^0 = X_q^m, \quad X_q^{m+1} = Y^{\mu^*}, \tag{45}$$

where μ^* is an integer such that, for a given small δ,

$$\left|\frac{Y^{\mu+1} - Y^{\mu}}{Y^{\mu+1}}\right| \le \delta \quad \text{for } \mu > \mu^*. \tag{46}$$

This procedure is repeated until, for a given small ε, the following holds:

$$\max_{1 \le i \le (N+1)(M+1)} \left|\frac{X_i^{m+1} - X_i^m}{X_i^{m+1}}\right| \le \varepsilon. \tag{47}$$

11. SOME RESULTS

Figure 3 presents the approximation for θ obtained for some given values of α, γ_1, γ_2, M, and N. The left side of each part presents the curves θ versus ξ (for $(N + 1)$ values of η) while the right side presents the curves and θ versus η (for $(M + 1)$ values of ξ). In this figure the dashed line represents the constant temperature approximation, obtained from Eq. (20).

Figure 4 presents a three-dimensional representation (θ as function of ξ and η) for four particular situations.

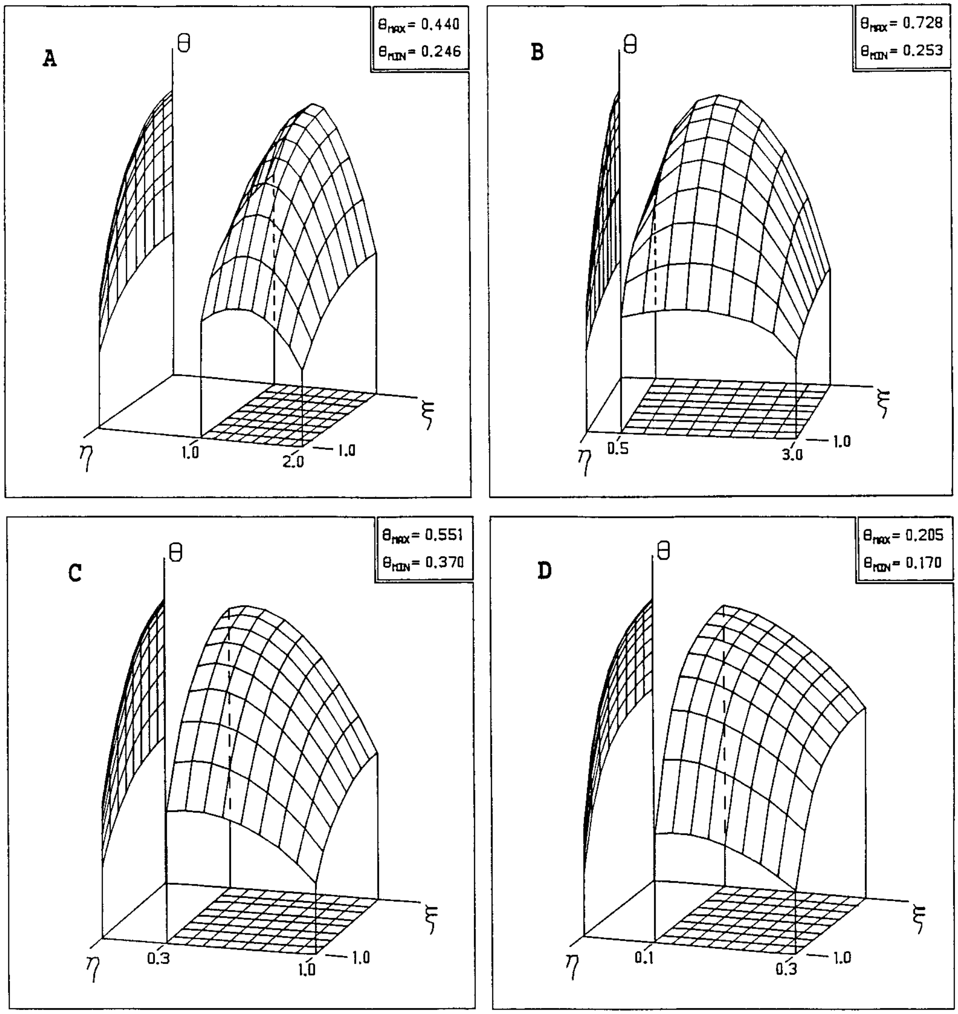

FIG. 4. The dimensionless temperature field θ as a function of ξ and η, obtained with $M = 8$ and $N = 8$ for $\alpha = 50.0$, $\gamma_1 = 1.0$, and $\gamma_2 = 2.0$ (part **A**), for $\alpha = 50.0$, $\gamma_1 = 0.5$, and $\gamma_2 = 3.0$ (part **B**), for $\alpha = 10.0$, $\gamma_1 = 0.3$, and $\gamma_2 = 1.0$ (part **C**) and for $\alpha = 100.0$, $\gamma_1 = 0.1$, and $\gamma_2 = 0.3$ (part **D**).

These results correspond to the minimization of $g^{p'}$ in which p' is an integer such that

$$\max_{1 \le i \le (N+1)(M+1)} \left| \frac{\Psi_i^{p'} - \Psi_i^{p'-1}}{\Psi_i^{p'}} \right| < 0.00001. \tag{48}$$

Figure 5 presents the sequence of intermediate solutions Ψ^1, Ψ^2, Ψ^3, Ψ^4, Ψ^5, and Ψ^6 as functions of ξ, the dimensionless radial position. This figure illustrates the convergence to θ.

The curve Ψ^1 versus ξ (first iteration) represents the approximation obtained without nonconvexity effects. The effect of the reemission from the body to itself may be observed by comparing the first iteration with subsequent iterations.

Figure 6 presents a comparison among four different approximations (obtained with different M and N) for a selected situation.

12. FINAL REMARKS

It is to be noticed that the constant temperature approximation becomes a good assumption when $\alpha \to 0$.

For instance, for $\alpha = 0.0001$, $\gamma_1 = 0.5$, $\gamma_2 = 1.0$, and $M = N = 8$ we have $\theta_{\max} = 7.268$ and $\theta_{\min} = 6.931$. Comparing the constant temperature approximation (given by Eq. (20)—in this case $\theta_c = 7.079$) with the finite element approximation (obtained with $M = N = 8$), the maximum relative error defined as

$$E_{\max} = \frac{\mathrm{MAX}\{|\theta_{\max} - \theta_c|, |\theta_c - \theta_{\min}|\}}{\theta_{\min}} \tag{49}$$

is less than 2.72%.

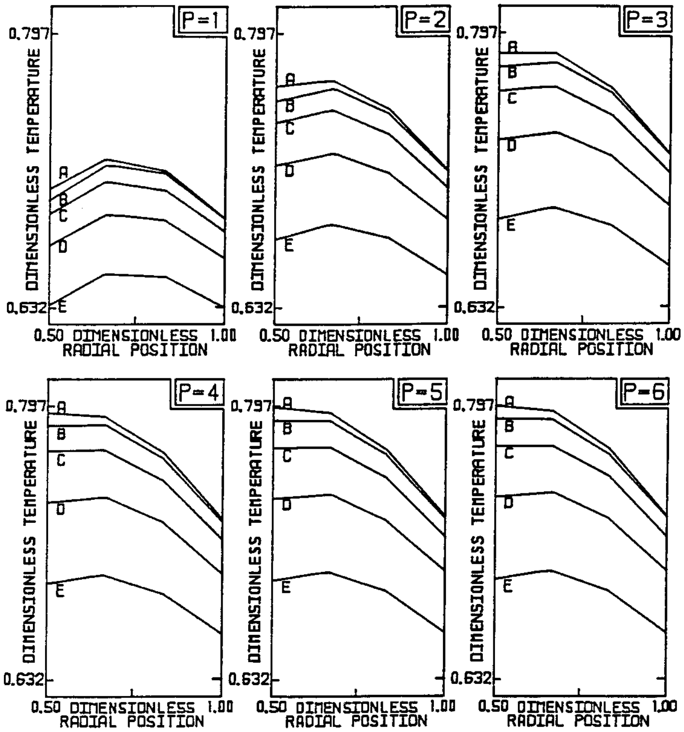

FIG. 5. The fields Ψ^p (for $p = 1$, $p = 2$, $p = 3$, $p = 4$, $p = 5$, and $p = 6$) versus the dimensionless radial position ξ (for $\eta = 0.000$ (A), $\eta = 0.250$ (B), $\eta = 0.500$ (C), $\eta = 0.750$ (D), and $\eta = 1.000$ (E)), obtained with $N = 4$ and $M = 3$ for $\alpha = 1.0$, $\gamma_1 = 0.5$, and $\gamma_2 = 1.0$.

On the other hand, if, instead of $\alpha = 0.0001$ we choose $\alpha = 10.0$ (in this case $\theta_{\max} = 0.475$, $\theta_{\min} = 0.358$, and $\theta_c = 0.398$), the maximum relative error ($E_{\max}$) is 21.5%. For $\alpha = 0.01$ we have $E_{\max} = 4.81\%$ and for $\alpha = 1.0$ we have $E_{\max} = 13.4\%$.

Some issues of convergence and accuracy may be discussed based on Figs. 5 and 6. In Fig. 5 it is easy to see that for $p = 5$ the convergence has been reached. In fact, for all the numerical simulations carried out (in addition to the ones presented in this work), the convergence was reached for $p \leq 10$. The worst case (among the ones simulated) was observed for $\alpha = 100.0$, $\gamma_1 = 0.1$, and $\gamma_2 = 0.3$ using $M = N = 6$. In such case the convergence (inequality (48)) was reached for $p = 10$.

The relation between accuracy and grid is illustrated in Fig. 6. In general, with $M = N = 6$, a good accuracy was observed in the simulations carried out.

APPENDIX I: EVALUATING THE ERROR IN THE ENERGY BALANCE

This work is concerned with a steady-state energy transfer process in a body with known internal heat generation surrounded by a vacuum. In other words, the amount of energy leaving the body by thermal radiation must be equal to the amount of energy generated in the body.

The energy, per unit time, generated in the body (in its dimensionless form) is given by

$$E_G = \int_\Omega 1\, dV = \pi(\gamma_2^2 - \gamma_1^2). \tag{AI.1}$$

The energy, per unit time, lost by thermal radiation (in its dimensionless form) is given by

$$\begin{aligned} E_R = {} & \left[\int_0^1 \alpha\theta^4 2\pi\gamma_1\, d\eta\right]_{\xi=\gamma_1} + \left[\int_0^1 \alpha\theta^4 2\pi\gamma_2\, d\eta\right]_{\xi=\gamma_2} \\ & + \left[\int_{\gamma_1}^{\gamma_2} \alpha\theta^4 2\pi\xi\, d\xi\right]_{\eta=1} \\ & - \left[\int_0^1\int_0^1 \alpha\theta^4 K^*(\eta,\eta')\, d\eta\, d\eta'\right]_{\xi=\gamma_1}. \end{aligned} \tag{AI.2}$$

If θ is the exact solution, E_R must be equal to E_G. In the cases where θ is obtained from a numerical approximation, the following quantity provides a measure of the numerical error in the energy balance

$$\Lambda = |E_G - E_R|/E_G. \tag{AI.3}$$

For instance, when $\alpha = 50.0$, $\gamma_1 = 0.5$, and $\gamma_2 = 3.0$ (in this case $E_G = 27.49$), the error "Λ" is given by

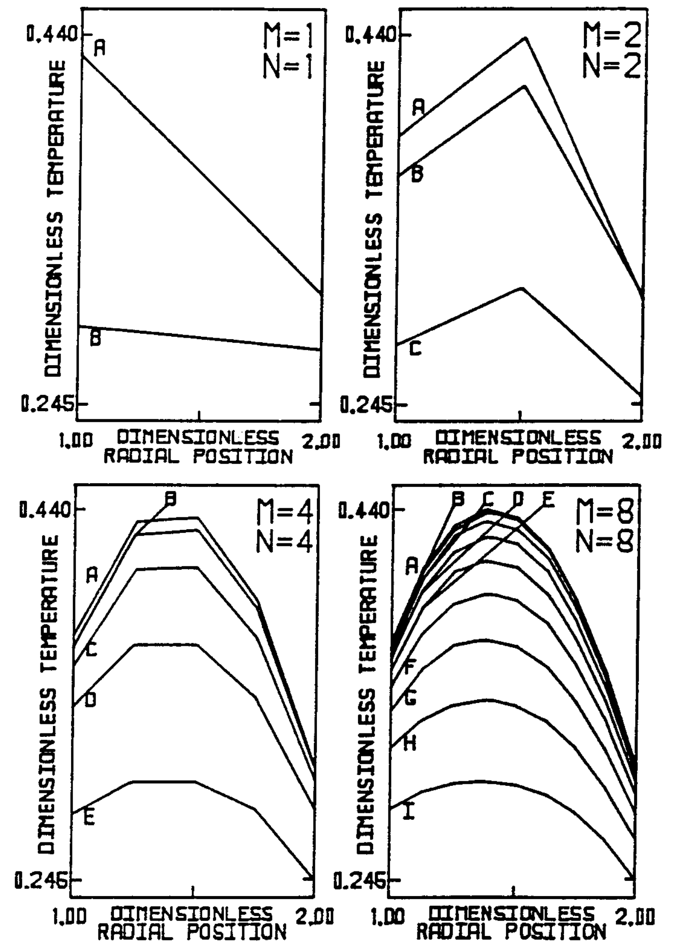

FIG. 6. Dimensionless temperature θ versus dimensionless radial position ξ obtained with $M = 1$ and $N = 1$ (for $\eta = 0.00$ (A) and $\eta = 1.00$ (B)), with $M = 2$ and $N = 2$ (for $\eta = 0.00$ (A), $\eta = 0.50$ (B), and $\eta = 1.00$ (C)), with $M = 4$ and $N = 4$ (for $\eta = 0.00$ (A), $\eta = 0.25$ (B), $\eta = 0.50$ (C), $\eta = 0.75$ (D), and $\eta = 1.00$ (E)) and with $M = 8$ and $N = 8$ (for $\eta = 0.00$ (A), $\eta = 0.125$ (B), $\eta = 0.25$ (C), $\eta = 0.375$ (D), $\eta = 0.50$ (E), $\eta = 0.625$ (F), $\eta = 0.75$ (G), $\eta = 0.875$ (H), and $\eta = 1.00$ (I)) for $\alpha = 50.0$, $\gamma_1 = 1.0$, and $\gamma_2 = 2.0$.

$$\Lambda = 0.0004 \quad (\text{when } M = N = 1) \qquad \text{(AI.4)}$$

$$\Lambda = 0.1810 \quad (\text{when } M = N = 2). \qquad \text{(AI.5)}$$

The error may be evaluated also from the difference between the energy, per unit time, generated in the body and the energy, per unit time, reaching the body boundary by conduction.

The energy, per unit time, reaching the body boundary (in its dimensionless form) is given by

$$E_C = \int_{\partial\Omega} -\operatorname{grad}\theta \circ \mathbf{n}\, dS. \qquad \text{(AI.6)}$$

If θ is the exact solution, then $E_C = E_G$. So the error Λ' may be defined as

$$\Lambda' = |E_G - E_C|/E_G. \qquad \text{(AI.7)}$$

For instance, when $\alpha = 50.0$, $\gamma_1 = 0.5$, and $\gamma_2 = 3.0$ (the same case considered above), the error "Λ'" is given by

$$\Lambda' = 0.7377 \quad (\text{when } M = N = 1) \qquad \text{(AI.8)}$$

$$\Lambda' = 0.4461 \quad (\text{when } M = N = 2). \qquad \text{(AI.9)}$$

The use of Λ and Λ' as an error estimate for numerical calculations may be unrealistic. This assertion may be illustrated as follows:

Suppose that $\alpha = 50.0$, $\gamma_1 = 0.5$, and $\gamma_2 = 3.0$. In this case, under the constant temperature approximation, the obtained dimensionless temperature is $\theta = 0.3287$.

Now, consider the linear problem

$$\frac{1}{\xi}\frac{\partial}{\partial \xi}\left(\xi \frac{\partial \overline{\theta}}{\partial \xi}\right) + \frac{\partial^2 \overline{\theta}}{\partial \eta^2} + 1 = 0, \quad \gamma_1 < \xi < \gamma_2, 0 < \eta < 1,$$
$$\overline{\theta} = 0.3287 \quad \text{for } \xi = \gamma_1, \xi = \gamma_2, \text{and } \eta = 1, \qquad \text{(AI.10)}$$
$$\frac{\partial \overline{\theta}}{\partial \eta} = 0 \quad \text{for } \eta = 0.$$

Evaluating E_R and E_C employing the exact solution of (AI.10) it is easy to see that

$$E_R = E_C = E_G \Rightarrow \Lambda = \Lambda' = 0. \qquad \text{(AI.11)}$$

Nevertheless, $\overline{\theta}$ is not a solution for (12).

REFERENCES

1. R. Siegel and J. R. Howell, *Thermal Radiation Heat Transfer,* 3rd ed. (Hemisphere, Washington, DC, 1992).
2. R. Fernandes and J. Francis, *J. Heat Transfer* **104,** 594 (1982).
3. C. E. Siewert and J. R. Thomas Jr., *J. Quant. Spectrosc. Radiat. Transfer* **48**(2), 227 (1992).
4. R. M. Saldanha da Gama, *J. Appl. Math. Phys.* **42,** (1991).
5. R. M. Saldanha da Gama, *J. Comp. Phys.* **99**(2), 310 (1992).
6. E. M. Sparrow and R. D. Cess, *Radiation Heat Transfer* (McGraw-Hill, Washington, DC, 1978).
7. R. M. Saldanha da Gama, J. A. O. Pessanha, J. A. R. Parise, and F. E. M. Saboya, *J. Solar Energy* **36**(6), 509 (1986).
8. K. Vafai and J. Ettefagh, *J. Heat Transfer* **110,** 1011 (1988).
9. G. Flamant, J. D. Lu, and B. Variot, *J. Heat Transfer* **116,** 652 (1994).
10. J. C. Slattery, *Momentum, Energy and Mass Transfer in Continua* (McGraw-Hill, New York, 1972).
11. R. M. Saldanha da Gama, *Appl. Math. Modelling* **14**(2) (1990).
12. B. N. Pshenichny and Yu. M. Danilin, *Numerical Methods in Extremal Problems* (MIR, Moscow, 1978).